**ONLINE APPENDIX**

# $P2Y_{12}$ Receptor Function and Response to Cangrelor in Neonates With Cyanotic Congenital Heart Disease

Elisabeth A. Kaza, MD,[a] Matthew C. Egalka, MD,[a] Hairu Zhou, MS,[a] Jianchun Chen, PhD,[a] Denise Evans, MSHS,[g] Jayne Prats, PhD,[g] Richard Li, PhD,[f] Scott L. Diamond, PhD,[f] Julie A. Vincent, MD,[b,c] Emile A. Bacha, MD,[d] Thomas G. Diacovo, MD[a,c,e]

## Inventory of Supplementary Information

Supplementary methods

1 supplementary table

1 supplementary figure and legend

Supplementary video legends

Supplementary references

## METHODS

**Reagents.** ADP and type 1 collagen (ChronoPar) were obtained from Chronolog (Havertown, PA). Human fibrinogen was purchased from Sigma Co. (Saint Louis, MO) and abciximab (αIIbβ3 inhibitor) from Centocor, Inc (Marvin, PA). The polyclonal anti-VWF antibody was purchased from Dako (Carpinteria, CA), the Alexa-488 conjugated anti-human CD61 (GPIIIa) antibody from Bio-Rad (Raleigh, NC), and the rabbit polyclonal anti-$P2Y_{12}$ antibody was from Alomone Labs (Jerusalem, Israel). The FITC-conjugated mouse anti-human monoclonal antibody CD42b (GPIbα), FITC-conjugated goat anti-rabbit polyclonal antibody, and FITC-conjugated mouse IgG1 (control) were from BD Biosciences (San Jose, CA). MAb 6D1 (function blocking antibody to human GPIbα) and cangrelor ($P2Y_{12}$ inhibitor) were kindly provided by Barry Coller (Rockefeller University, NY) and The Medicine Company (Parsippany, NJ).

**Flow Cytometry.** 50 μL of freshly isolated human platelets (1 x $10^8$ / mL) suspended in platelet buffer (PB; 145 mmol/L NaCl, 10 mmol/L Hepes, 0.5 mmol/L $Na_2HPO_4$, 5 mmol/L KC1, 2 mmol/L $MgCl_2$, 0.1% glucose, pH 7.4) containing 50 ng/mL of prostaglandin E1 (Sigma, St. Lois, MO) were aliquoted into U-bottom microtiter plates (Linbro-Titertek Flow Labs, McLean, VA) containing either control, anti-$P2Y_{12}$, anti-CD42b, or anti-CD61 antibody (final conc. 10 μg/mL). After 15 min of incubation at room temperature (RT), an additional 100 μL of PB was added, platelets pelleted, supernatant removed, and pellets resuspended in 100 μL of PB. After 10 min of resting, PB containing 2% paraformaldehyde (100 μL) was added. After 30 min, samples were centrifuged, washed and resuspended in 100 μL of PB containing 2.5 mM EGTA. For samples pre-incubated with anti-$P2Y_{12}$ antibody, 1μL of FITC-conjugated goat anti-rabbit

polyclonal antibody was added (30 min, RT). All samples were then diluted to 200 µL and analyzed on a FACs Calibur flow cytometer (BD, Franklin Lakes, NJ) using CELLQuest software, version 6.0. The platelet population was identified by its forward and side scatter distribution and 20,000 events were analyzed for mean fluorescence.

**Platelet Aggregation.** Purified platelets were suspended to a final concentration of 400,000 / µl in PB. Stock solutions of cangrelor were prepared on the day of experimentation and added to platelet suspensions 10 min prior to inducing aggregation with ADP (5 µmol/L or 20 µmol/L). Human fibrinogen (final concentration 200 µg/ml) and $CaCl_2$ (final concentration 1 mmol/L) were added to the platelet suspensions just prior to activation. Aggregation was assessed using a Chronolog Lumi-Aggregometer (model 540 VS, Chronolog, Havertown, PA) and permitted to proceed for 6 min (37°C, 1,200 rpm) after the addition of agonist. The results are reported as maximum percent change in light transmittance from baseline with platelet buffer used as a reference (mean ± SEM). The concentration of ADP inducing 50% of maximal aggregation (EC50) was calculated by GraphPad Prism software (version 6.00 CA, USA) from a concentration-response curve obtained with ADP concentrations ranging between 0.63 µmol/L and 20 µmol/L. The concentration of cangrelor inhibiting 50% of maximal platelet aggregation (IC50) induced by ADP (5 µmol/L or 20 µmol/L) was also calculated by GraphPad Prism software from concentration-effect curves obtained with cangrelor concentrations ranging between 0.012 nmol/L and 116 nmol/L. All data was normalized to aggregation in the absence of drug (mean ± SEM).

**Platelet adhesion in flow.** A parallel-plate flow chamber was used to assess platelet accumulation on surface-immobilized plasma VWF at a wall shear rate of 1,600 $s^{-1}$ (29-31). In brief, a polyclonal anti-VWF antibody was absorbed overnight (4°C) to a six-well tissue culture plate. Subsequently, the plate was washed and nonspecific interactions blocked by the addition of PB containing 3% HSA, pH 7.4 (30 min, 37°C). Heparinized whole blood was used to generate either human plasma or plasma VWF $^{HA1}$, which was then added to the plates and incubated at 37°C for an additional 1 h prior to use. Citrated whole blood was then perfused over the reactive substrate for 3 minutes, followed by the addition of platelet buffer with or without ADP (20 mmol/L) for 1 min. Of note, GPIbα–VWF interactions are cation-independent, and thus are capable of forming in the presence of citrate, while integrin αIIbβ3 requires the presence of cations for full activity. For GPIbα inhibition studies, mAb 6D1 (10 μg/ml) was added to anticoagulated human blood for 10 min before use. Platelet accumulation and translocation were visualized (10X and 20X objective lens, respectively) using an automated inverted microscope system (DMI6000, Leica) equipped with a CCD camera (DFC365FX, Leica). The number of platelets attached per unit area was determined by offline analysis (ImagePro Plus, Media Cybernetics, Bethesda, MD) of recorded digital images.

Microfluidic devices with 8 individual channels (250 μm wide x 60 μm-high) were fabricated in polydimethylsiloxane (PDMS) as previously described (32). The device was reversibly vacuum-sealed to a glass slide with its flow channels aligned perpendicularly to a patterned type 1 collagen surface (1 mg/ml). To visualize platelet accumulation over time, an Alexa Fluor 488 conjugated, non-function blocking mouse anti-human CD61 (αIIb/β3) antibody was added (1:50 ratio) 7 min prior to performing experiments (0.125 μg/ml final concentration). PPACK-treated whole blood from neonates with single ventricle pathology or healthy adults was

perfused over the prothrombotic surface at an initial wall shear rate of 100 $s^{-1}$ by withdrawal from a single outlet into a syringe pump (Harvard Apparatus Pump 11 Elite, Holliston, MA). Platelet accumulation was visualized (10X objective lens) using an automated inverted microscope system (DMI6000, Leica) equipped with a CCD camera (DFC365FX, Leica). A custom stage insert held three microfluidic devices allowing replicate testing of four conditions. Images were captured in 30 s intervals for a total of 10 min. Platelet fluorescence intensities, which are directly proportional to the total platelet mass were measured and analyzed with Image J software (Image J; NIH, Bethesda, MD). The center 65% of the prothrombotic region was selected for analysis to avoid edge effects. The initial image was taken as background and subsequent images were background corrected. Platelet adhesion and aggregate formation was not observed upstream or downstream of the collagen trip prior to full channel occlusion.

***In vivo* thrombus formation.** Administration of anesthesia, insertion of venous and arterial catheters, fluorescent labeling of human platelets, and surgical preparation of the cremaster muscle in 12 week old male VWF $^{HA1}$ mice have been previously described (29). Purified human platelets (700K/μL) were continuously infused (25 μL/min) through a catheter placed in the ipsilateral femoral artery 2 min prior to and during laser-induced injury to ensure a level of circulating cells equivalent to humans (30). Injury to the vessel wall of arterioles (40-65 μm diameter) was performed with a pulsed nitrogen dye laser applied through a 20X water-immersion Olympus objective. Human platelet-vessel wall interactions were visualized by fluorescence microscopy using a system equipped with a Yokogawa CSU-22 spinning disk confocal scanner, iXON EM camera, and 488-nm laser line (Revolution XD, Andor Technology, South Windsor, CT) to detect Calcein-AM-labeled cells. After establishing a baseline for normal

thrombus generation in injured arterioles, cangrelor was then given as an intravenously bolus (30 μg/kg) followed by a continuous infusion (4 μg/kg/min) (25, 27). In a given animal, 6 thrombi (2 pre- and 4 post-infusion of cangrelor) were induced either upstream of the previous thrombi or in a different arteriole within the same cremaster preparation. The extent of thrombus formation was assessed for 2 min after injury. Maximal area ($\mu m^2$) and the median integrated fluorescence signal of platelets (function of time and area) were determined by off-line analysis using SlideBook 6 (Intelligent Imaging Innovations, Denver, Colorado).

**Statistics.** Results are shown as mean ± SEM from experiments conducted with blood from different donors. Statistical analysis was performed using a Mann-Whitney U test and one-way analysis of variance (ANOVA) with the Bonferroni post-test to determine significance among curve fits for multiple data sets. All data were analyzed using GraphPad Prism software (version 6.00 CA, USA). Values of $p < 0.05$ were considered statistically significant.

**Supplemental Table 1. Baseline characteristics of patients with shunt thrombosis from September 2013 through September 2016[#]**

| | |
|---|---|
| Total number of patients with shunt thrombosis | 11 |
| Mean age at shunt palliation (days) | 13.4 ± 5.7 |
| Female - no. (%) | 3 (27.3) |
| Male - no. (%) | 8 (72.7) |
| Weight at shunt palliation (kg) | 2.9 ± 0.4 |
| Gestation (weeks) | 38 ± 1.7 |
| Congenital cardiac defect - no. (%) | |
| Hypoplastic left heart syndrome | 5 (45.5) |
| Pulmonary atresia with intact ventricular septum | 1 (9.1) |
| Tetralogy of Fallot with pulmonary atresia | 1 (9.1) |
| Tricuspid atresia | 0 |
| Heterotaxy syndromes | 2 (18.2) |
| Other single-ventricle defect | 1 (9.1) |
| Other two-ventricle defect | 1 (9.1) |
| Type of initial systemic-to-pulmonary-artery shunt - no. (%) | |
| Modified Blalock-Taussig shunt | 8 (72.7) |
| With Norwood procedure | 3 (27.3) |
| Without Norwood procedure | 5 (45.4) |
| Right ventricular-to-pulmonary shunt | 0 |
| With Norwood procedure | 0 |
| Without Norwood procedure | 0 |
| Central shunt | 3 (27.3) |
| Need for ECMO after shunt thrombosis - no. (%) | 8 (72.7) |
| Death (pts) | 6 (54.5) |
| Death from cardiovascular cause | 6 (54.5) |
| Death related to cardiac procedure | 0 |
| Death from non-cardiovascular cause | 0 |
| Heart transplantation | 0 |
| Shunt thrombosis - no. (%)[*] | |
| Decreased murmur and increased cyanosis | 9 (81.8) |
| Impairment of shunt flow (Echo, catheterization) | 4 (36.4) |
| Postmortem observation | 0 |
| Progressive cyanosis requiring shunt revision (OR) or revascularization procedure | 3 (27.3) |
| Progressive cyanosis requiring chest opening in the NICU | 2 (18.2) |

[#]Values are means ± SD.

*Shunt thrombosis was confirmed by detection of one or more of the following: decreased murmur and increased cyanosis; impairment of shunt flow observed on echocardiography; postmortem; progressive cyanosis requiring urgent shunt revision in the OR or revascularization procedure; or progressive cyanosis requiring chest opening in the NICU.

**Supplemental Figure 1**

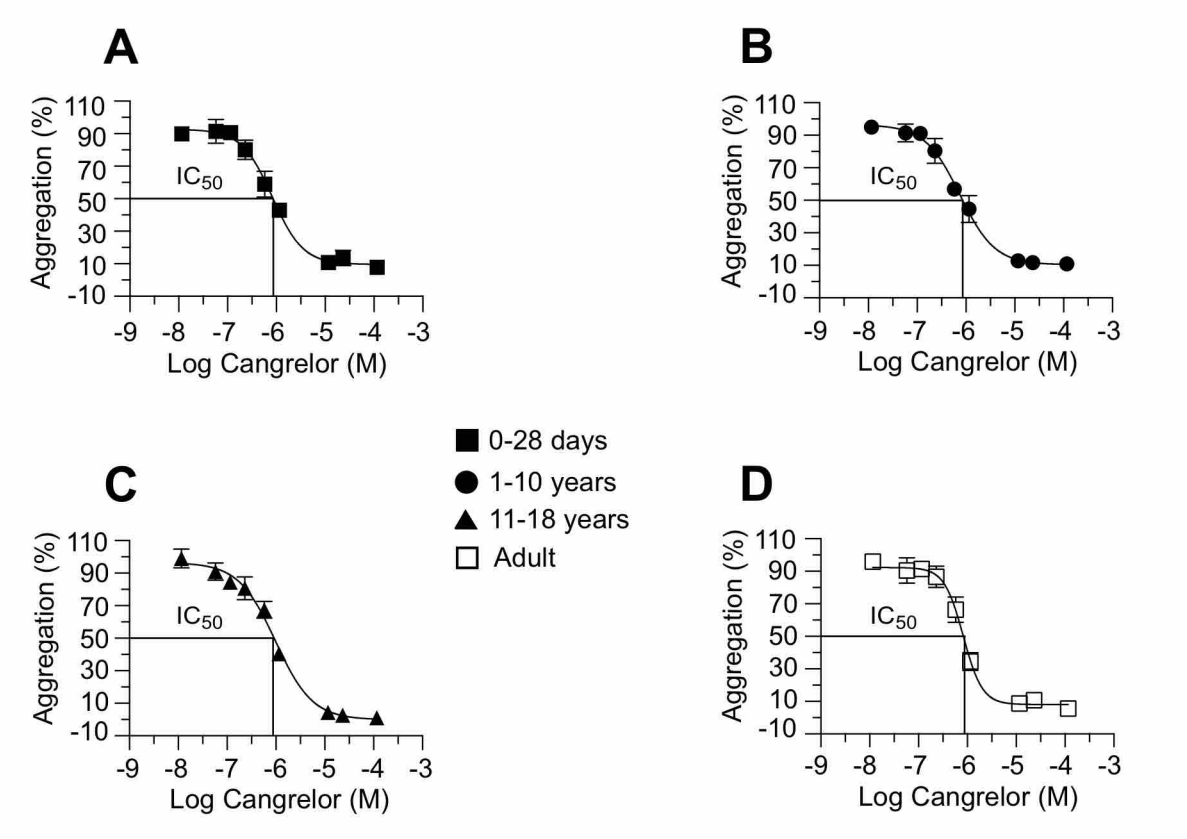


**Effect of Cangrelor on Platelet Aggregation in Response to ADP. (A-D)** Concentration response curves for the determination of IC50 values for cangrelor (5 µmol/L ADP) as measured by LTA using purified platelets from neonatal and pediatric patients with congenital heart disease or healthy adult volunteers. Concentrations of the cangrelor are plotted in Log form. Results are the mean ± SEM; n = 12 (0 - 28 days); n = 7 (1 - 10 years); n = 7 (11 - 18 years); n = 12 (adults).